**Proceedings of International Collaboration on Advanced Neutron Sources (ICANS-VII), 1983 September 13-16**
**Atomic Energy of Canada Limited, Report AECL-8488**

# PROGRESS IN MATERIALS INVESTIGATIONS FOR SNQ - TARGETS

P. Krautwasser *
W. Lohmann **

Kernforschungsanlage Jülich GmbH, D-5170 Jülich, FRG
* Division for Reactor materials (IRW)
** Solid State Division (IFF-SNQ)

## Summary

The materials investigations and development program for heavily loaded components of the SNQ-target wheel is presented. This broad program includes the target elements, proton beam windows, the slide ring sealing and the water chemistry of the cooling systems. Two examples are discussed as highlights in more detail: the thermal cycling effects on uranium (part of the target element development) and the possible use of sinter aluminium product for the stationary proton beam window.
During thermal cycling of uranium alloys at a lower temperature of 55°C and temperature differences $\Delta T$ = 10, 35 and 65 K, the growth rate per cycle approaches at higher cycle numbers a constant value for each $\Delta T$. The growth rate increases with increasing $\Delta T$ and seems to be less influenced by differences in uranium alloy composition or material microstructure than by the amplitude of the temperature cycle.

## Introduction

The achievement of a safe and reliable operation of the SNQ-target wheel introduces to a great extent new requirements to be met by the used materials. This holds especially for heavily loaded components from irradiation effects and from thermomechanical stresses; Fig. 1 shows such components, which therefore must be investigated in detail.

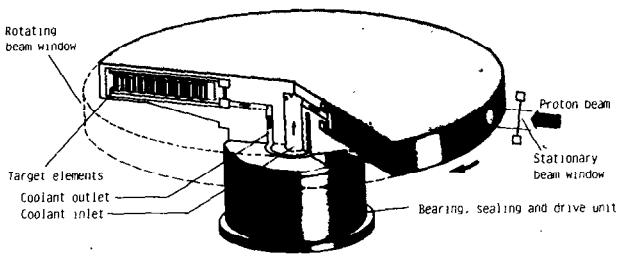


Fig. 1:
The SNQ-target wheel and its components exposed to intense irradiation and high thermomechanical load

A corresponding materials testing, qualification and development program has been worked out and is depicted in Tab. 1.
The most extensive task is the target element development, where three operational target elements based on Pb, W, and U are the ultimate goal. Problem areas do not only exist for the target material itself - particularly for the U-case -, but also concerning the development of a reliable combination of target material - bonding - cladding (preferably Al). The investigations dedicated to the cladding material will also reveal useful data for the rotation proton beam window and the general structural material of the target wheel.

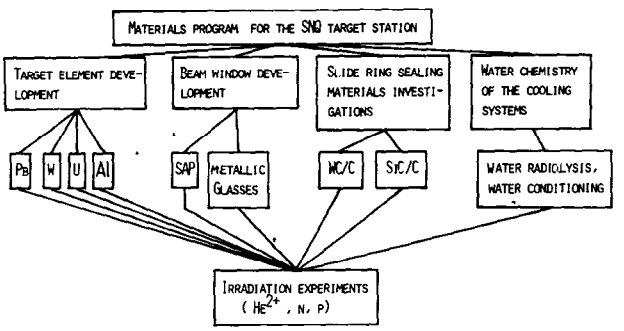


Tab. 1:
SNQ-target station materials program and promising materials for the different applications

The highest materials performance is required for the stationary proton beam window, which is considered as a desirable, but not imperatively needed component. The emphasis is presently put on materials with extremely high irradiation resistance; Al-alloys like sinter aluminium product (SAP) and metallic glasses with high thermal stability like $Nb_{40}Ni_{60}$ seem to be promising.
Because of the unusual SNQ-operating conditions, the concern in the case of the slide ring sealing materials is the applicability of conventional combinations (WC/C); hence, also new developments, e.g. SiC/C have been included.
The water chemistry investigations are primarily devoted to radiolysis and concomitant enhanced corrosion effects under intense proton- and neutron irradiation. The data evaluated hereby are the basis of a technical design for the water conditioning systems and of the operations parameters to be set and controlled.
All branches of this material program end up in irradiation experiments, which are described in detail elsewhere (Lohmann, 1983). Their basic idea is a staged procedure from simulation experiments with He-implantation or n-irradiation to a variety of experiments under conditions at least close to SNQ, which are performed at the LAMPF-proton accelerator (800 MeV/1 mA). Their final step will be the proof test of a complete small target wheel.
In order to illustrate the recent progress of this program, two examples - one of the target element development and another of the beam window development - are discussed below in more detail.

## Thermal cycling of Uranium

### Purpose of Study

By increasing the effective target area, the rotating target planned for SNQ reduces the thermal load for a specific target area by a factor of 200, i.e. increases the cooling period from $10^{-2}$ (proton pulse frequency: 100 Hz) to 2 sec compared to a stationary target with the same proton beam power. This leads to a far lower operation temperature for the rotating target. Both, lower temperature and longer cooling period reduces the thermal cycling growth rate of alpha-uranium, as discussed later. Although the operation temperature and the cycle frequency, i.e. number of cycles during target wheel operation ist reduced, requirements for spallation materials, bondings and claddings are still high.
The lower operation temperatures $T_o$ and the amplitude of thermal cycling $\Delta T$ of an uranium target for the first and second stage of SNQ are $T_o \leq 160°C$, $\Delta T \leq 65$ K (350 MeV, 5 mA) and $T_o = 125°C$, $\Delta T = 65$ K (1100 MeV, 5 mA) respectively. The corresponding data for the initially considered first stage of 1100 MeV and 0.5 mA were $T_o = 55°C$ and $\Delta T = 10$ K. For the orthorhombic alpha-uranium with a highly anisotropic thermal expansion coefficient, the interaction of adjacent grains leads to high local stresses and plastic strain during thermal cycling and thus to thermal cycling growth.
A number of studies mainly by Mayfield, 1958, Zegler, 1958, Lloyd, 1958, and Pugh, 1956, shows a relationship between thermal cycling growth and lower temperatur $T_o$, $\Delta T$, heating and cooling rate, time at temperature and material texture. The available data for alpha-uranium cycling groth were measured in a temperature range above 350°C and are therefore not applicable for SNQ temperatures (Fig. 2).

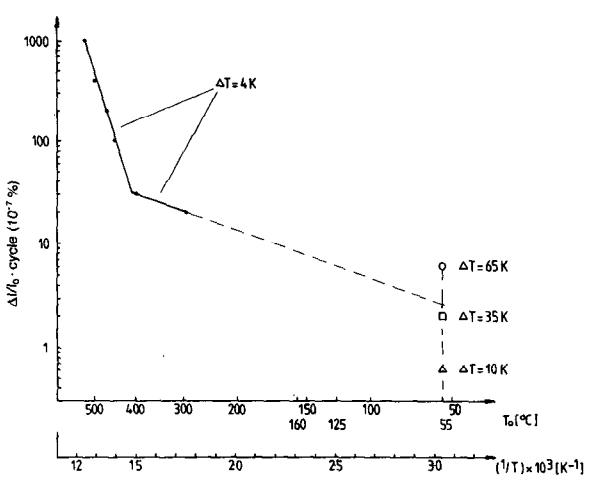


Fig. 2:
Extrapolation of thermal cycling growth data ($\Delta T$ = 4 K) by Mayfield, 1958, and results of this study

To investigate the influence of thermomechanical cycling on the behaviour of the specific materials to be used for the SNQ target under conditions relevant for SNQ, three techniques are used: 1. thermal cycling by immersion of samples in liquids of different temperatures and automatic sample transfer, 2. thermal cycling of samples by inductive heating and water cooling in a medium frequency furnace (4 kHz) and 3. simulation of thermal cycling by high cycle fatigue. First results of method /1/ will be reported in this paper.

Measurements of thermal cycling growth at lower operation temperatures of the SNQ variants $T_o$ of 55, 125, and 160°C and cycling temperatures $\Delta T$ of 10, 35, 65, 100 K, will provide the functional relationship of cycling growth with $T_o$ and $\Delta T$ (Table 2) for four uranium alloys. Subsequently, the effect of time at temperature will be studied.

| Lower temperature $T_o$ (°C) | Temperature Amplitude $\Delta T$ (K) | | | |
|---|---|---|---|---|
| 55 | +10 | +35 | +65 | |
| 125 | | +35 | +65 | +100 |
| 160 | | +35 | +65 | +100 |

Tab. 2:
Lower temperatures and temperature differences of the cycling program

### Experimental

To study thermal cycling growth at a lower temperature of $T_o = 55°C$ and temperature amplitudes of $\Delta T$ = +10, +35, + 65, four thermostats with liquid-temperatures of 55, 65, 90 and 120°C were used. The samples were transferred between the two corresponding thermostats by an electronically controlled, pneumatic driven sample handler. Stabilized polydimenthylsiloxane (BAYSILONE-M 50) was used as liquid. Time at temperature (sample immersion time) was 15 sec each, to keep the temperature difference between the liquid and the center of the sample under 12% of $\Delta T$. With a transfer time of 2-2.5 sec, the total cycle period was 35 sec.
At intervals of about $1.5 \cdot 10^4$ cycles, the length and weight of the samples were measured.

### Samples

For the first study, four uncladded uranium-alloys "off the shelf", machined to cylinders of 9.0 mm diameter and 50 mm in length were used:
pure uranium, U - 5 W/o Mo, U - 3.7 W/o Zr, U - 0.75 W/o Ti.

### Results

The weight loss of the uncladded samples due to corrosion is shown in Fig.3 as a function of the number of cycles, i.e. time, for $\Delta T$ = 10, 35 and 65 K. Up to $6 \cdot 10^4$ cycles the measurements were performed in air, later on in nitrogen. Pure uranium had the highest corrosion rate, followed by the U - 3.7 W/o Zr alloy. U - 0.75 W/o Ti and U - 5 W/o Mo showed the lowest weight loss. In all cases, the corrosion rate was proportional to $\Delta T$.
Assuming a uniform surface corrosion, a correction factor for the sample length was calculated from the weight loss of a sample. From the difference in sample lenght at a given number of thermal cycles and the original length of the uncycled sample and in consideration of the correction factor the thermal cycling growth per cycle ($\Delta l/l_o \cdot$cycle) was calculated. The results for the cycling amplitude of $\Delta T$ = 10 K is shown in Fig. 3. The scale of the ordinate ($10^{-7}$ %), provides $\Delta l/l_o$ in % for an operation-time of the target of about one year ($10^7$ cycles).
At low cycle numbers, the different alloys show distinct variations, caused in part by the normalization of $\Delta l/l_o$ to a small number of cycles, in part by non-typical dimensional changes due to internal stresses introduced by sample machining. At cycle numbers higher than $10^5$, the mean thermal cycle growth rate per cycle reaches a constant value and seems to be fairly independent on alloy composition or sample microstructure with a somewhat lower value for pure uranium.

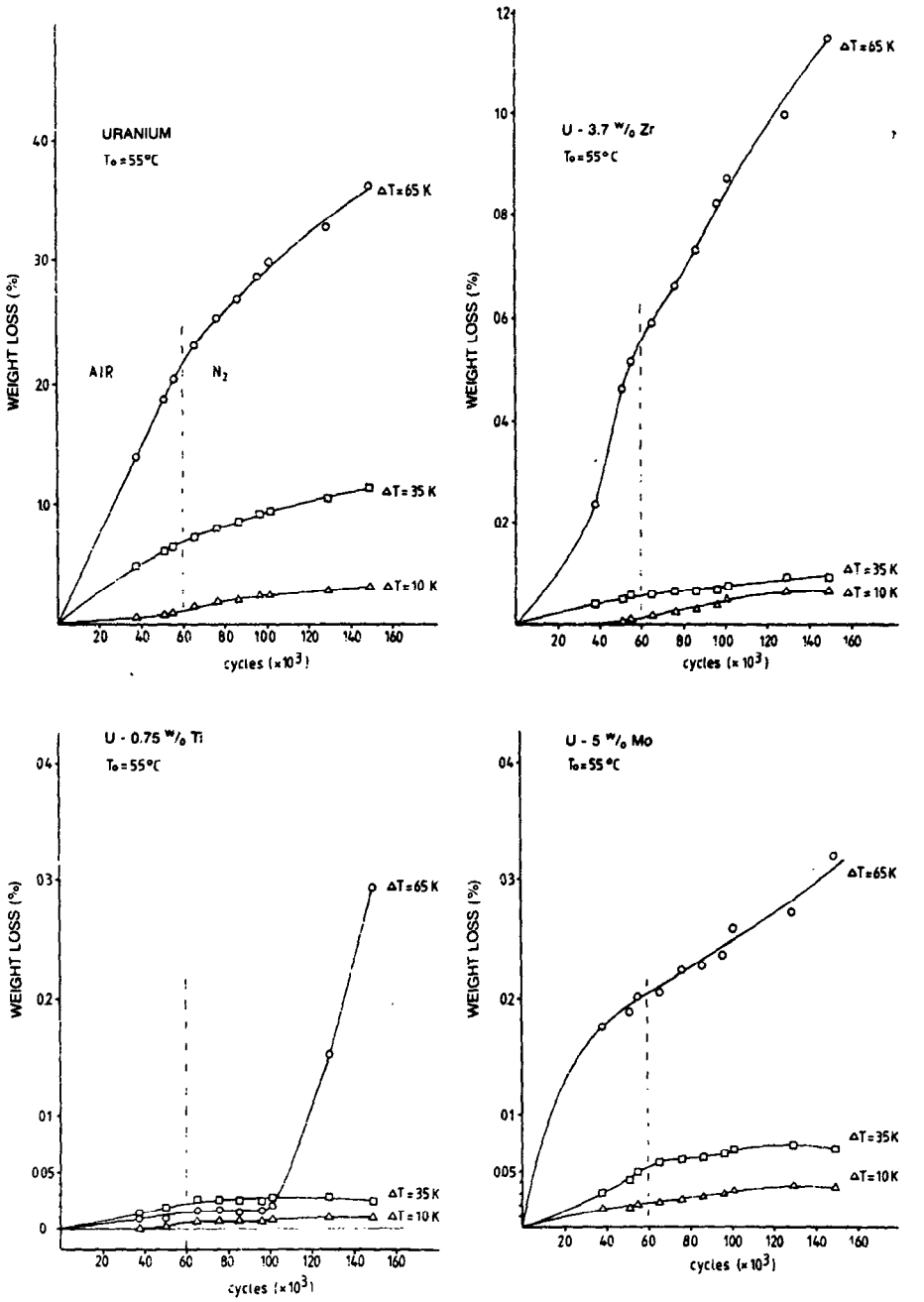


Fig. 3:
Weight loss of uncladded uranium alloys during thermal cycling

Except for pure uranium, the same is true for the three uranium alloys cycled at $\Delta T = 35$ K shown in Fig. 4.
Fig. 5 shows the corresonding growth rates for a cycling amplitude of $\Delta T = 65$ K. Again pure uranium yields a somewhat higher value than the uranium alloys, which seem to converge at $15 \cdot 10^4$ cycles to about the same growth rate per cycle.
A comparison of the results listed in table 3 shows an increase in thermal cycling growth with increasing $\Delta T$.

| Alloy composition | $\Delta l / l_0 \cdot$ cycle $(10^{-7}$ %) | | | | | |
|---|---|---|---|---|---|---|
| | $\Delta T$ = 10 K | | $\Delta T$ = 35 K | | $\Delta T$ = 65 K | |
| Uranium | -1.4 | ≦ 0.6 | 6.1 | ≦ 2.0 | 8.5 | ≦ 6.0 |
| U-3.7 w/o % | -0.1 | | 1.1 | | 5.7 | |
| U-5 w/o % | 0.6 | | 2.0 | | 4.7 | |
| U-0.75 w/o % | 0.2 | | 1.6 | | 3.4 | |

Tab. 3:
Thermal cycling growth rates at $1.5 \cdot 10^5$ cycles and at a lower temperatur $T_0 = 55$°C and $\Delta T$ of 10, 35, and 65 K

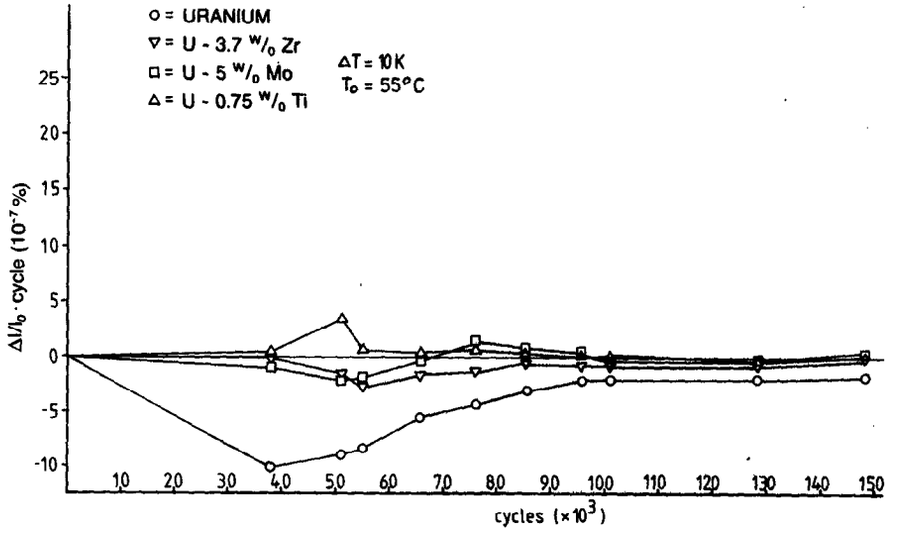


Fig. 4:
Thermal cycling growth per cycle at a lower temperature of 55°C and a cycling amplitude of + 10 K

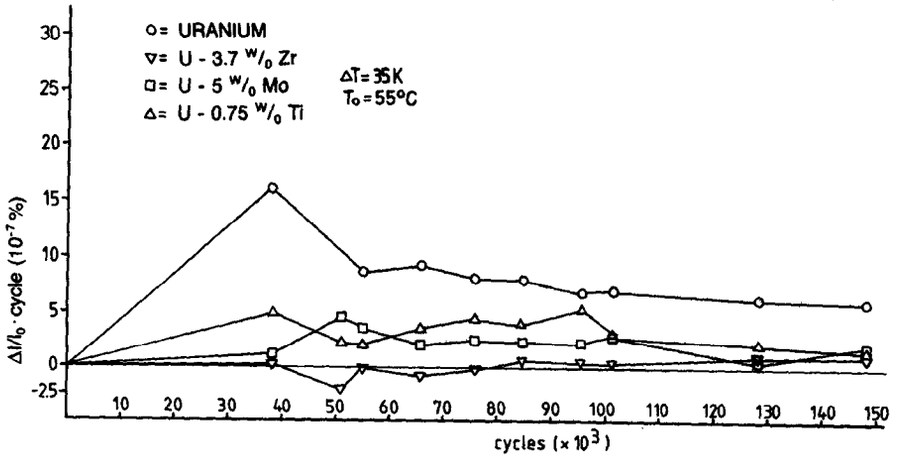


Fig. 5:
Thermal cycling growth per cycle at a lower temperature of 55°C and a cycling amplitude of + 35 K

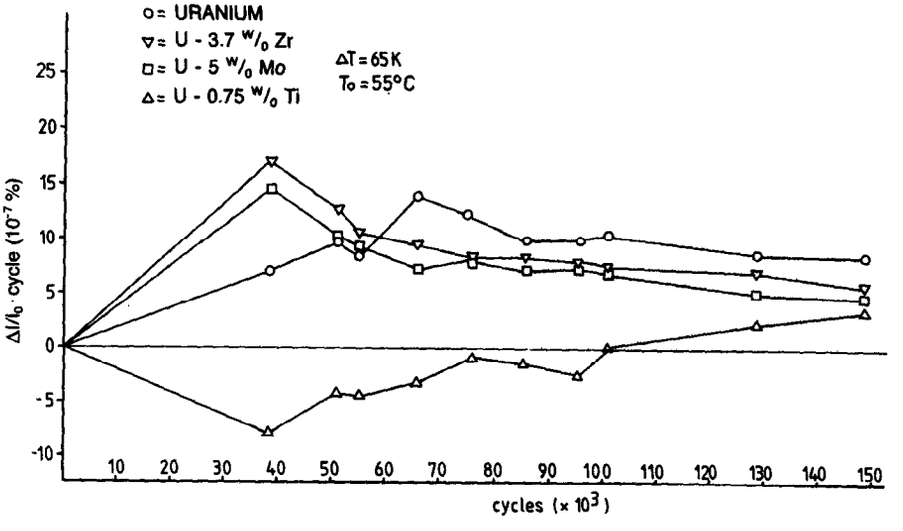


Fig. 6:
Thermal cycling growth per cycle at a lower temperature of 55°C and a cycling amplitude of + 65 K

In Fig. 4 through 6 $\Delta l/l_0$ per cycle is the mean value of the growth rate at a given total cycle number, leading to smaller systematic errors at higher cycle numbers. In contrast to this, the data shown in Fig. 7 are the mean values of the growth rate per cycle of cyle number intervals of about $2 \cdot 10^4$ cycles. Although the scatter is larger, the growth rate per cycle seems to be constant for cycle numbers larger than $8 \cdot 10^4$. The growth rate date for the basic temperatures of $T_0$ = 125 and 160°C are expected to be higher according to Mayfield, 1958 (Fig.2). In addition, the higher cooling rate of 2 sec of the target wheel compared to 15 sec in our test facility may increase the growth rate to some extend (Mayfield, 1958), although the cooling rate of the rotating target is still lower than the cooling rate of a stationary target.

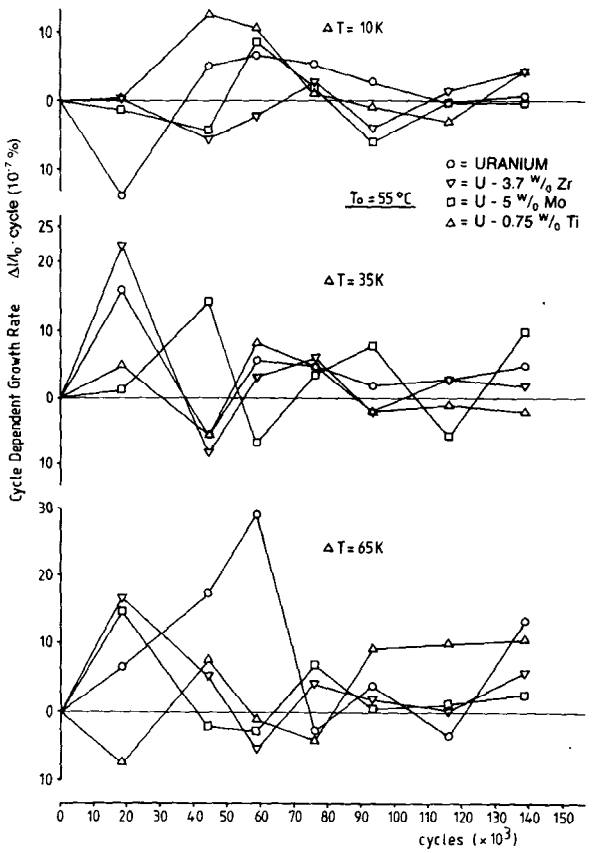


Fig. 7:
Growth rates per cycle calculated for subsequent cycle number intervals of about $2 \cdot 10^4$ cycles

## Beam window development

### SAP-AlMgSi-composite alloy

There are three essential requirements for the stationary proton beam window (cf Fig. 1):
- sufficient strength at elevated temperatures,
- both low heat production and proton radiation damage favouring thus material with low atomic and mass number,
- acceptable technological properties.

Al-based alloys seem to be promising from this point of view. One has further to distinguish between sintered and usual, wrought material.
The sintered alloy SAP (Al-matrix + 7 % $Al_2O_3$) has reasonable strenght up to 400°C and - more important - shows no He-/H-embrittlement up to 1700 appm each at least for high-oxide SAP (Maziasz, 1979). On the other hand, SAP is a brittle material with poor technological properties (e.g. weldability).
AlMgSi-alloys - chosen as general structural material for the target wheel - are limited to an upper operations temperature below 150°C. A high irradiation resistance is known from neutron irradiations (Farrell, 1979), but there are no data on proton irradiation effects with the concomitant high He- and H-production. These Al-alloys are ductile and possess good and well known technological properties.
Combination of the favourable properties of both materials led to the development of a SAP-AlMgSi-composite alloy, consisting of a SAP core surrounded by an AlMgSi-border. Preliminary tests on prototype disks reveal a good quality of the transition zone from optical metallography and a high gas-tightness, indicated by a leakage-rate of less than $10^{-9}$ mbar·l·s$^{-1}$ at 200°C.

### Radiation effects on Al-based alloys

Calculations have been performed for the case of a proton beam power of 0.6 MW (1100 MeV, 0.5 mA, prev.first SNQ-stage) assuming equal damage effects for SAP and pure Al. The results are compiled in Table 4.

| | Displacement rate (dpa/sec) | He-production rate (appm He/sec) | H-production rate (appm H/sec) |
|---|---|---|---|
| Protons | $2.2 \times 10^{-7}$ | $7.3 \times 10^{-5}$ | $3 \times 10^{-4}$ |
| Fast neutrons | $1.4 \times 10^{-8}$ | $2.6 \times 10^{-13}$ | $2.4 \times 10^{-13}$ |
| Total | $2.3 \times 10^{-7}$ | $7.3 \times 10^{-5}$ | $3 \times 10^{-4}$ |

Tab. 4:
Radiation damage of an Al-based stationary proton beam window for 0.6 MW proton beam power

The neutron contribution to the total damage can be neglected. At least for high-oxide SAP, a theoretical window lifetime of about 6.500 h is possible from the He-produktion rate; the corresponding dpa-damage is less than 6 dpa, which should not affect the materials integrity (H-embrittlement) because of a high H-diffusivity at SNQ-operating temperatures (see below).

### Stress and temperature considerations for SAP

A simple assessment of the mechanical and thermal load on a SAP-based beam window has been made assuming a double-disk plate geometry as depicted in Fig. 8.
The maximum temperature $T_{max}$ can be estimated (Lohmann, 1982) from the energy balance, inserting a coolant temperature of 300 K and assuming a heat transfer coefficient of 1 W/(cm$^2$·K). The time-averaged power density from beam heating turns out to be about 500 W/cm$^3$ for a 0.6 MW proton beam power.
The maximum stress $\sigma_{max}$ from bending moments is calculated (Lohmann, 1982) as a fuction of the window thickness d and the pressure differential p (1 and 3 bar, resp.). Results are shown in Fig. 9, together with the expected maximum temperature $T_{max}$.
The $T_{max}$-values corresponding to a given d are indicated on the upper scale. Referring to this scale, the temperature-dependent yield strength $\sigma_{0.2}$ (T) and the ultimate tensile strength $\sigma_{UTS}$ (T) of SAP - 7 % $Al_2O_3$ has also been drawn in. The intersection of the strenght curves with $\sigma_{max}$ (T,p) denotes the minimum thickness $d_{min}$ at a fixed p. The corresonding data can be read from the insert of Fig. 9, assuming $\sigma_{max} \leq \sigma_{0.2}$ (T).

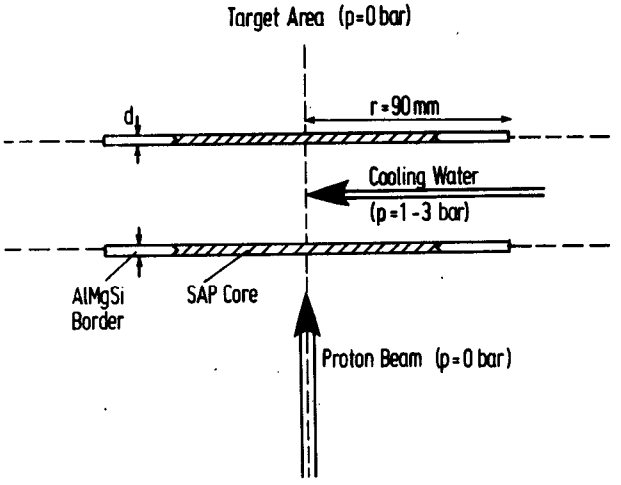


Fig. 8:
Internally water cooled, double-disk plate beam window with thickness d and plate radius r = 90 mm, determined by the proton beam size

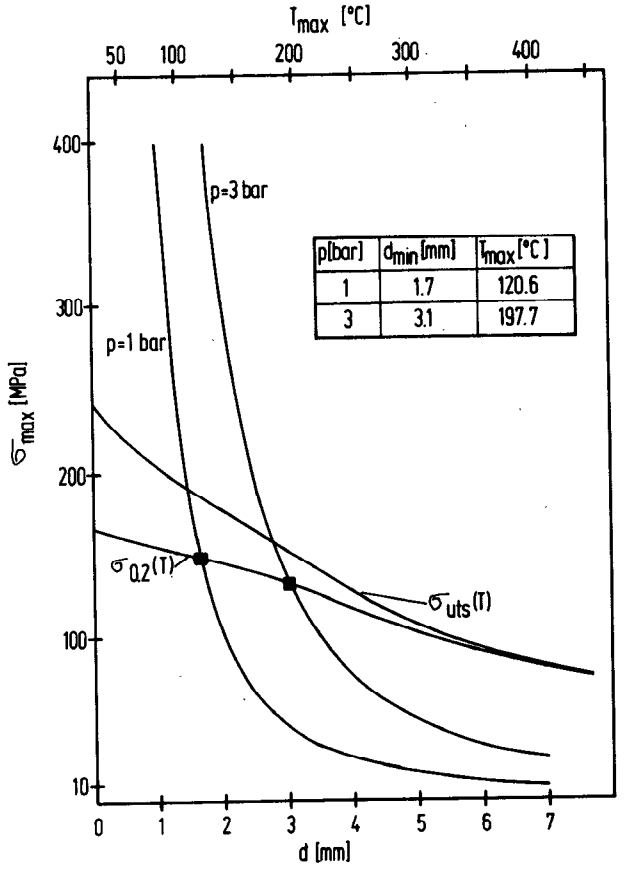


Fig. 9:
Evalution of the needed beam window plate thickness d from stress and temperature calculations (see text)

From these results, a moderate operations temperature combined with sufficient strenght is indicated. Ongoing investigations will deal with irradiation effects from He and proton irradiations. The He-experiments are dedicated to the change of mechanical properties of preimplanted material as a function of its $Al_2O_3$-content, because there is a ductility improvment by a lower oxide fraction. The LAMPF proton irradiation tests (Lohmann, 1983) will be performed on complete proton type disks under operating conditions close to SNQ. Additionally, Al-C has been included into the current program as an alternative Al-based sintered alloy offering a substantially higher ductility than SAP, but with the lack of data on its irradiation behaviour.

## References

Farrell, K.; King, R.T.
"Tensile Properties of Neutron Irradiated 6061 Aluminium Alloy in Annealed and Precipitation-Hardened Conditions"
Proc. Conf. on Effects of Radiation on Structural Materials, ASTM-STP 683 (1979), 440

Lloyd, L.T.; Mayfield, R.M.
"Microstructural Changes of Uranium upon Thermal Cycling"
Trans. Amer. Soc. Metals, 50 (1958), 954

Lohmann, W.; Hammad, F.M.
"On the Possibility of Using Sintered Aluminium Product (SAP) as a Beam Window Material for SNQ-I"
Technical Note SNQ (August 1982)

Lohmann, W.
"Irradiation Effects in Candidate Materials for the SNQ-Target Station"
Proc. ICANS-VII (1983), this volume

Mayfield, R.M.
"Effects of Cycling Variables upon Growth Rate of 300°C Rolled Uranium"
Trans. Amer. Soc. Metals, 50 (1958), 926

Maziasz, P.J.; Farrell, K.
"The Tensile Properties of High Oxide SAP Containing Helium and Tritium"
J. Nucl. Mat. 85+86 (1979), 913-917

Pugh, S.F.
"Radiation Damage in Fissile Materials"
Progr. Nucl. Energy, Ser. V, 1 (1956), 652-671

Zegler, S.T.; Mayfield, R.M. and Mueller, M.H.
"Effects of Fabrication and Heat Treatment Variables upon the Thermal Cycling Behaviour of Uranium"
Trans. Amer. Soc. Metals, 50 (1958), 905